Distance Estimation Using Bidirectional Communications Without Synchronous Clocking

Chih-Yu Wen,* Robin D. Morris,† and William A. Sethares*

February 4, 2006

Abstract

A fundamental problem when locating sensors in a network is to estimate the distance between pairs of sensors. This paper considers a variety of time-of-arrival and phase-shift approaches that use bidirectional signalling to bypass the need for accurate synchronous clocking. The measurement techniques are simulated and analyzed to assess the accuracy of the distance estimation. The analysis demonstrates trade-offs between the accuracy of the oscillators, the accuracy of the subsequent distance estimation, and the complexity of the methods.

EDICS: SEN-COLB Collaborative Signal Processing; SPC-DETC Detection, Estimation, and Demodulation.

1 Introduction

Sensor location estimation is required in many sensor network applications [1]-[5]. Due to the low power, lower cost, and simple configuration requirements of wireless sensor networks, GPS devices, accurate synchronous clocks, and the installation of a base station may be precluded. However, when all sensors can measure the range to their neighbors, accurate relative location estimates are possible [6]-[13].

This paper investigates two methods for distance measurement using bidirectional communications: (1) Distance Estimation via Asynchronous Clocks (DEVAC) and (2) Distance Estimation via Asynchronous Phase Shift (DEVAPS).

*The authors are with the Department of Electrical and Computer Engineering, University of Wisconsin-Madison, Madison, WI 53706 USA. {chihyu_wen@yahoo.com.tw and sethares@ece.wisc.edu}

†RIACS, NASA Ames Research Center, MS 269-2, Moffett Field, CA 94035-1000. {robin.morris@gmail.com}

The DEVAC method operates analogously to a pulsed radar in which a signal is bounced from the target and the distance is determined by how long it takes the signal to return. Since sensors are typically small and operate with low power; the signal cannot bounce from the receiver. Instead, the target sensor receives the transmission and sends a reply that acts analogously to the return of the radar. The DEVAPS method operates analogously to a continuous wave radar in which a sinusoidal signal is bounced from the target. In this case, the distance is determined by the phase shift between the signal and its rebound. Though the individual distance measurements are ambiguous, the ambiguity can be resolved by repeating the procedure with different wavelength carriers. Thus the sensors operate cooperatively (bidirectionally) in order to synthesize a signal that acts like the reflection in a radar system.

In order to understand the behavior of the network, it is also necessary to measure the accuracy of the estimation [14]-[16]. This paper presents an estimation-theoretic analysis of the proposed measurement mechanisms to assess the achievable estimation accuracy. Specifically, quantitative expressions are provided to demonstrate the operation of the DEVAC method, and the Cramer-Rao Bound on phase and frequency accuracy are computed to show the limits of performance with the DEVAPS method.

The analytical portions of this paper assume that only the line-of-sight (LOS) path exists. However, in real radio channels, there may exist multiple transmission paths between the sensors. In order to investigate the effect of this multipath interference on the distance estimations, the performance is evaluated in two multipath environments as detailed in Section 6.2.

The rest of the paper is organized as follows: Section 2 provides a brief literature review on range-measurement techniques. Section 3 describes and analyzes the DEVAC method using bidirectional communication between sensors to establish time stamps that correctly adjust for asynchronies in the clocks. Section 4 presents the DEVAPS method which measures the time indirectly using the phase of a carrier signal; an analysis of the estimated phase error using either a ML estimator or a phase-locked loop is derived to examine the accuracy of the distance estimation. Section 5 explores the trade-offs of the distance measurement using the DEVAC and DEVAPS methods given the same energy consumption. Section 6 provides an overall comparison and investigates the behaviors of the different methods using signals in several frequency bands. The performance is presented via simulations and numerical examples considering measurement errors from several sources such as timing resolution, processing delay, and clock calibration in the DEVAC method and phase and frequency estimation accuracy in the DEVAPS method. The simulations verify the approximate Gaussian distributions of the range measurements using DEVAC and DEVAPS methods and examine the multipath contributions to the performance of the respective methods. The final section concludes and discusses

variations of the proposed ranging techniques.

2 Related Work

The distances between pairs of transceivers in a sensor network may be determined by using time of arrival (TOA), angle of arrival (AOA), or received signal strength (RSS) measurements of signals with RF-based [17]-[19],[29],[30], [32]-[34], acoustic [20],[21],[31], or ultra-wideband [22]-[24] techniques. Overviews of techniques for ranging can be found in [25] and [26].

Many methods of distance measurement use one-way communication to estimate distances between pairs of sensors that typically require time synchronization or accurately characterized path loss models. Time-of-arrival techniques often require that the transmitter and receiver are synchronized in time; the transmitter places a time stamp on the transmission and sends that to the receiver which can then estimate the distance [27]. The range estimation technique in [21] does not need to maintain accurate clocks, but it does require a post synchronization stage [28] to achieve calibration and reduce estimation errors. In [19], the distance is estimated by measuring the received signal strength. Though received signal strength methods tend to give biased answers, the sensor can utilize channel models to optimize the overall system performance and the method can reduce the average range error significantly. [29] proposes the radio interferometric positioning system (RIPS), which exploits interfering radio waves emitted from two locations at slightly different frequencies and uses the relative phase offset of the signal at the receivers to obtain the necessary ranging information for localization. However, an external synchronization strategy is necessary to align the start of the transmission and reception at multiple sensors.

On the other hand, bidirectional communication ranging [30]-[34] provides an opportunity to invoke a calibration step (e.g. timing calibration) and employ techniques to adjust the variations in transceiver characteristics (e.g. correct latencies induced by system components) within the estimation procedures. That is, pairs of sensors can determine distances through bidirectional communication and information sharing to improve ranging accuracy in a low-precision environment without synchronous clocking. A spread spectrum method for direct sequence ranging systems using two-way measurements is given in [30]. This operates by counting the number of chips offset between the local and received code sequences. This limits the range resolution to a chip period and a distance measurement is accurate to within a time span of 1/2 chip, which means the higher chip rate (i.e. the higher timing resolution), the higher range-measurement accuracy. [33] uses a handshaking protocol to measure the round-trip travel time (RTT). When

wishing to update its position, a sensor transmits a direct-sequence request-to-send (RTS) waveform. Neighboring sensors which hear the RTS respond simultaneously with acknowledgement (ACK) direct-sequence waveforms. Then the initialing sensor estimates the TOAs of all signals from neighboring sensors to measure the distances. However, the performance may be limited by multiple access interference (MAI) in CDMA systems. In order to solve the MAI problem, [34] presents channel estimation and distributed algorithms for localization in a wireless ad hoc network. A direct-sequence CDMA-based handshaking protocol and the generalized successive interference cancellation/matching pursuits (GSIC/MP) algorithm are used to obtain RTT and AOA measurements for the geolocation problem in the multiuser environment.

3 Direct Distance Estimation

The most straightforward method of estimating the distance between sensors directly measures the time required for a signal to propagate between the sensors. For low-powered sensors where the communication range is limited to a few hundred meters, the distance must be estimated to sub-meter accuracy. When transmitting with electromagnetic signals, one meter of distance corresponds to a time delay of approximately $3ns$. This requires extremely accurate clocks that are precisely synchronized. Such clocks may be more expensive than desired in the network application.

3.1 Distance Estimation via Asynchronous Clocks (DEVAC)

The DEVAC method helps to alleviate the need for highly accurate synchronous clocking. Suppose that sensors A and B are equipped with clocks (oscillators) that are assumed to be asynchronous in both frequency and phase. Denote t_i^a and t_j^b as the time stamps in sensors A and B, respectively; let t_{del}^a and t_{del}^b be the delay time in sensors A and B, respectively; t_{ab} is the signal propagation time. The estimation proceeds as shown in Figure 1:

a. Sensor A transmits a message containing the time t_0^a (the time indicated on its clock at the start of the transmission).

b. Sensor B receives the first message at time t_2^b (which is t_{ab} seconds after it is transmitted).

c. Sensor A transmits a second message containing the time t_1^a (the time indicated on its clock at the start of the second transmission).

d. Sensor B receives the second message at time t_3^b (which is also t_{ab} seconds after it is transmitted).

e. Sensor B calibrates its clock to A's using the differences $t_1^a - t_0^a$ (which is known from A's message) and $t_3^b - t_2^b$ (the arrival times).

f. Some time t_{del} later, sensor B transmits the time $t_{del}^a = z \cdot t_{del}^b$ that has elapsed since reception of A's message along with the time stamp t_4^b (the time on B's clock when it transmits). These times are adjusted (if necessary) using the scale factor $z = \frac{t_1^a - t_0^a}{t_3^b - t_2^b}$.

g. Sensor A receives the reply when its clock reads t_5^a. The transmission time t_{ab} can be calculated as

$$t_{ab} = \frac{t_5^a - t_1^a - t_{del}^a}{2}.$$

Though this method shows that time delay estimation is possible without synchronous clocking, it suffers from the drawback that the clocks must be very accurate, able to measure time differences in the nanosecond range.

3.2 Analysis of the DEVAC Method

This section analyzes the accuracy of the distance measurement as a function of the accuracy of the clock by deriving an approximate distribution for the estimation based on the DEVAC method of Figure 1. The random variable T represents the sensor estimate of the true *t*; thus T_{ab} is an estimate of the true time t_{ab} and T_i^a is the estimate of the time t_i^a as measured by the clock of sensor A. The estimated transmission time is

$$T_{ab} = \frac{T_5^a - T_{del}^a - T_1^a}{2}. \tag{1}$$

Since sensor B calibrates its clock to A's using time differences,

$$T_{del}^a = Z \cdot T_{del}^b, \tag{2}$$

where

$$T_{del}^b = T_4^b - T_3^b, \tag{3}$$

$$Z = \frac{T_1^a - T_0^a}{T_3^b - T_2^b} \tag{4}$$

is a scale factor that represents how much faster or slower clock A moves than clock B.

For the purpose of analysis, assume that all measurements T_i^a and T_j^b are independent normal random variables with the same variance σ^2 caused by the measurement error in the clock:

$$T_i^a \sim N(t_i^a, \sigma^2) \quad \text{for } i = 0, 1, 5. \tag{5}$$

$$T_j^b \sim N(t_j^b, \sigma^2) \quad \text{for } j = 2, 3, 4. \tag{6}$$

This normality assumption is justified in [27] when the clock skew is small.

Hence the random variable Z is the ratio of two normal random variables. As shown in [35] and [36], under reasonable conditions on the distributions, Z is well approximated by

$$Z \sim N(\mu_Z, \sigma_Z^2) \tag{7}$$

with

$$\mu_Z = \frac{\mu_1}{\mu_2}$$

and

$$\sigma_Z^2 = \frac{2\sigma^2}{\mu_2^2}\left(1 + \left(\frac{\mu_1}{\mu_2}\right)^2\right),$$

where $\mu_1 = t_1^a - t_0^a$ and $\mu_2 = t_3^b - t_2^b$. For this Gaussian approximation to hold, μ_2 must be biased away from zero and the ratio μ_2/σ^2 must be large. These are reasonable assumptions in the sensor communication application.

From (2) and (7), T_{del}^a can be viewed as the product of two normal random variables. Since the measurement errors are small, [37] shows that the distribution of T_{del}^a can be sensibly approximated by

$$T_{del}^a \sim N\left(\mu_Z t_{del}^b, 2\mu_Z^2\sigma^2 + {t_{del}^b}^2\sigma_Z^2\right) \tag{8}$$

when μ_Z/σ_Z and $\mu_{T_{del}^b}/\sigma_{T_{del}^b}$ are large, which is a reasonable assumption in this case.

Using the above analysis and referring to (1), the distribution of T_{ab} is

$$T_{ab} \sim N\left(\mu_{T_{ab}}, \sigma_{T_{ab}}^2\right), \tag{9}$$

where

$$\mu_{T_{ab}} = \frac{1}{2}(t_5^a - \mu_Z t_{del}^b - t_1^a)$$

and

$$\sigma_{T_{ab}}^2 = \frac{1}{4}\left[(2 + 2\mu_Z^2)\sigma^2 + {t_{del}^b}^2\sigma_Z^2\right].$$

Note that the mean of random variable T_{ab} is the true value of the transmission time between sensors A and B and the variance of T_{ab} depends on the variance of the timing measurement σ^2, the characteristic of the clock-adjustment factor (4), and the time delay t_{del}^b.

Finally, the distribution of the distance measurement D_{ab} is given by

$$D_{ab} \sim N\left(c\mu_{T_{ab}}, c^2\sigma^2_{T_{ab}}\right) \tag{10}$$

since the transmission distance is the product of the transmission speed c and the transmission time. Observe that the mean of random variable D_{ab} is the true value of the distance, showing that the estimator is unbiased. Numerical results are presented in Section 6.1.

Results from [38]-[40] relate the accuracy of synchronous distance estimates to the signal-to-noise ratio (SNR) and the effective bandwidth of the signal. The expression in (10) is the added inaccuracy due to the asynchronous clocking mechanism. Equation (10) shows the distribution of the distance estimates when using a single transmitted pulse. One way to increase the clock accuracy is to use k different estimates. If they are independent, the resulting estimation is then

$$\hat{D}_{ab} \sim N\left(c\mu_{T_{ab}}, \frac{c^2\sigma^2_{T_{ab}}}{k}\right). \tag{11}$$

4 Using Phase Shift to Measure Distance

Though the DEVAC method does not require synchronous clocks, it does require highly precise time stamps. The following methods, Distance Estimation via Asynchronous Phase Shift 1 and 2 (DEVAPS1 and DEVAPS2), relax this by using the phase of a carrier signal in a bidirectional communication aimed at estimating the distance.

4.1 Distance Estimation via Asynchronous Phase Shift (DEVAPS)

Suppose that sensors A and B are equipped with transmitters that operate at the same nominal carrier frequency. Suppose also that they contain a method of determining the phase difference between the carrier of the received signal and the internal reference oscillator. For example, this may be a phase-locked loop [41] or a Costas loop [42], or it may be some more complex system (e.g. maximum likelihood, ML) capable of estimating the phase and frequency offsets [43]. In the case of a software-defined radio [44], the speed of estimation may be traded-off against the required computations. There is also a power trade-off since faster estimation means that the signal may be transmitted for a shorter time.

The time delay estimation procedure of the DEVAPS1 method is shown diagrammatically in Figure 2, where time is designated in terms of the phase of the carrier signal. This method does not require that the oscillators at sensors

A and B have exactly the same frequency. The heart of the method is that sensor B can modify the frequency of its carrier (and use this modified frequency for subsequent transmission) to match the actual frequency f of the oscillator at sensor A. On the other hand, the best B can do is to estimate f. Any errors in this estimation will cause errors in the ultimate estimate of t_{ab}. For example, the error that will accrue in the phase over the time t_{del} (i.e., the time after the reception from A ceases and before the transmission from B begins) is directly proportional to the number of cycles in t_{ab} times the error in frequency. It is important, therefore, to keep this time short.

This method can only estimate the phase difference up to a multiple of 2π. This results in an ambiguous distance measurement $ct_{ab} + n\lambda$ where c is the speed of signal propagation, λ the wavelength of the carrier wave, and n an arbitrary integer. For example, with a carrier frequency $f = 100$ MHz and c the speed of light, the wavelength λ is about 3 meters. The sensors may be 10 meters apart, 13 meters apart, or $10 + 3n$ for any integer n. This is shown in the top line of Figure 3.

The following methods can be used to remove the ambiguity from the distance estimates:

1. The procedure of Figure 2 can be repeated using a different carrier frequency f_2, where f and f_2 are not commensurable (Two nonzero real numbers *n* and *m* are said to be commensurable if n/m is a rational number.). The distance can then be estimated by combining the two measurements into a single (relatively) unambiguous estimate of the distance. This is shown in Figure 3, where the arrow points to the region where the distance most likely lies. Observe that lower frequencies, which have longer wavelengths, may be preferred.

2. The received signal strength can be used to obtain a rough estimate of the distance, which can be used to eliminate the bulk of the ambiguity. This is discussed further in Section 6.1.

3. Network information can be used to avoid ambiguity. For instance, estimations from multiple pairs of sensors can be combined to give better estimates.

If the sensors are capable of transmitting and receiving at the same time (presumably on a different carrier frequency f_2), then errors due to the phase drift during t_{del} can be eliminated. This "full-duplex" version of the DEVAPS method, DEVAPS2, is shown in Figure 4.

a. Sensor A transmits a carrier signal at frequency f_1, $\cos(2\pi f_1 t + \phi_a)$, where ϕ_a is a known reference phase. (Again, $\phi_a = 0$ is the simplest choice.)

b. Sensor B receives the signal, as $\cos(2\pi f_1 t + \phi_a + 2\pi f_1 t_{ab})$.

c. Sensor B phase locks its local oscillator to the received signal or estimates the phase $\phi_a + 2\pi f_1 t_{ab}$ and frequency f_1 of the received signal. (This may be done using a PLL, a Costas loop, a ML estimator, or any other appropriate method.)

d. Sensor B generates a new carrier at f_2 that is mode locked to f_1. (This is feasible when $f_2 = \frac{n}{m} f_1$ for small integers n and m.) B then transmits a signal with carrier f_2. The transmitted signal is $\cos(2\pi f_2 t + \frac{n}{m}(\phi_a + 2\pi f_1 t_{ab}))$.

e. Sensor A receives the signal as $\cos(2\pi f_2 t + \frac{n}{m}(\phi_a + 2\pi f_1 t_{ab}) + 2\pi f_2 t_{ab})$.

f. Sensor A uses a phase (and frequency) matching algorithm to measure the phase difference, which is $2\pi \frac{n}{m} f_1 t_{ab} + 2\pi f_2 t_{ab}$. Since n,m, f_1 and f_2 are known, sensor A can compute t_{ab} and hence the distance d.

The (second) carrier at frequency f_2 must be simply related to f_1 so that B's oscillator can lock to the received f_1 and easily generate a mode locked version of f_2. The mode locking of oscillators is discussed at length in [45].

As with the DEVAPS1 method, the DEVAPS2 method returns ambiguous estimates which must be disambiguated using one of the strategies outlined above. The use of two mode-locked frequencies in the DEVAPS2 method is very different from (and not a substitute for) the use of two incommensurable frequencies in the disambiguation process. The primary advantage of the DEVAPS2 method is that it reduces the error in the frequency estimation to (approximately) zero. Thus, it gives more accurate distance estimations. On the other hand, more complex circuitry is required in the sensor since it must be capable of receiving and transmitting simultaneously.

4.2 Analysis of the DEVAPS2 Method Using a ML Estimator

There are several methods for estimating the frequency and phase of a sinusoidal signal observed in additive white Gaussian noise. This analysis adopts an approximate maximum likelihood (ML) estimator as detailed below to describe the performance of the distance measurement using the DEVAPS2 method and assumes that the oscillator noise is small. A discussion of the effects of oscillator noise may be found in [46]-[50].

The frequency f_0 and phase ϕ of a sinusoidal signal embedded in white Gaussian noise can be estimated using the data set

$$x[n] = \cos(2\pi f_0 n + \phi) + w[n] \quad n = 0, 1, 2, \ldots, N-1, \tag{12}$$

where $0 < f_0 < \frac{1}{2} f_s$, f_s is the sampling frequency, and $w[n] \sim N(0, \sigma_n^2)$. Denoting $\mathbf{x} = [x[0], x[1], \ldots, x[N-1]]^T$

and $\theta = [f_0, \phi]^T$, the likelihood function is

$$p(\mathbf{x}|\theta) = \frac{1}{(2\pi\sigma_n^2)^{\frac{N}{2}}} \exp\left[-\frac{1}{2\sigma_n^2}\sum_{n=0}^{N-1}(x[n] - \cos(2\pi f_0 n + \phi))^2\right]. \tag{13}$$

Thus, the maximum likelihood problem for estimating θ becomes

$$\text{minimize} \quad \sum_{n=0}^{N-1}(x[n] - \cos(2\pi f_0 n + \phi))^2 \tag{14}$$

$$\text{subject to} \quad 0 < f_0 < \frac{1}{2}f_s. \tag{15}$$

In [51], an approximate ML estimator of θ is given by

$$\hat{f}_0 = \arg\max_f \frac{1}{N}\left|\sum_{n=0}^{N-1} x[n]\exp(-j2\pi f n)\right|^2 \tag{16}$$

$$\hat{\phi} = \arctan\frac{-\sum_{n=0}^{N-1} x[n]\sin 2\pi\hat{f}_0 n}{\sum_{n=0}^{N-1} x[n]\cos 2\pi\hat{f}_0 n} \tag{17}$$

with

$$\sigma^2_{\hat{f}_0} \geq \frac{3}{\pi^2\gamma N(N^2-1)} \tag{18}$$

$$\sigma^2_{\hat{\phi}} \geq \frac{2(2N-1)}{\gamma N(N+1)}, \tag{19}$$

where γ is the SNR ($1/2\sigma_n^2$). For a large data set, the ML estimator is asymptotically efficient and optimal since it is asymptotically unbiased and achieves the Cramer-Rao lower bound.

Assume that sensor A transmits a sinusoidal signal $\cos(2\pi f_1 t + \phi_{a_1})$. Sensor B receives A's message embedded in white Gaussian noise and applies a ML estimator to determine the frequency and phase of the received signal, $\hat{f}_1$ and $\hat{\phi}_b$, where $\hat{\phi}_b = \phi_{a_1} + 2\pi f_1 t_{ab} + \triangle\phi_b$ and $\hat{f}_1 = f_1 + \triangle f_1$, where $\triangle\phi_b$ and $\triangle f_1$ are estimation errors. On the basis of this frequency estimation $\hat{f}_1$, sensor B generates a new frequency $f_2^{'} = \frac{n}{m}\hat{f}_1$ and transmits $\cos(2\pi f_2^{'} t + \frac{n}{m}\hat{\phi}_b)$ to sensor A. After receiving the signal as $\cos(2\pi f_2^{'} t + \frac{n}{m}\hat{\phi}_b + 2\pi f_2^{'} t_{ab})$ with noise, sensor A applies a ML estimator to match the phase and frequency. This yields

$$\hat{\phi}_{a_2} = \frac{n}{m}\hat{\phi}_b + 2\pi f_2^{'} t_{ab} + \triangle\phi_{a_2}, \tag{20}$$

where $\triangle\phi_{a_2}$ is the phase measurement error.

Using the DEVAPS2 method and assuming $\phi_a = 0$, the phase difference is

$$\hat{\phi}_{a_2} = 2\pi\frac{n}{m}f_1 T_{ab} + 2\pi f_2 T_{ab}, \tag{21}$$

where T_{ab} is the estimate of transmission time. Hence,

$$T_{ab} = \frac{m}{4\pi n f_1}\hat{\phi}_{a_2} \quad (22)$$

$$= t_{ab} + \frac{m}{4\pi n f_1}\left[2\pi\frac{n}{m}\triangle f_1 t_{ab} + \frac{n}{m}\triangle\phi_b + \triangle\phi_{a_2}\right]. \quad (23)$$

From the asymptotic normality theorem [52], the distribution of T_{ab} can be approximated by

$$T_{ab} \sim N(\mu_{T_{ab}}, \sigma^2_{T_{ab}}) \quad (24)$$

with

$$\mu_{T_{ab}} = t_{ab}$$

and

$$\sigma^2_{T_{ab}} = \frac{1}{(4\pi f_1)^2\gamma N(N+1)}\left[2(2N-1)(1+(\frac{m}{n})^2) + \frac{24t^2_{ab}}{N-1} - 12t_{ab}\right],$$

where γ is the SNR and *N* is the number of samples of the received signal. The variance of T_{ab} depends on the carrier frequency f_1, the SNR, the number of samples N of the received signal, the ratio n/m, and the real transmission time t_{ab}. Note that the approximation in (24) using the asymptotic normality theorem assumes the best possible performance of the frequency and phase estimator, which is an optimal characterization of T_{ab}.

Thus, the distribution of the estimated distance using f_1 with wavelength λ_1 is

$$D_{f_1} \sim N(c\mu_{T_{ab}} + l\lambda_1, c^2\sigma^2_{T_{ab}}) \quad (25)$$

and the distribution of the estimated distance using f_2 with wavelength λ_2 is

$$D_{f_2} \sim N(c\mu_{T_{ab}} + l\lambda_2, c^2\sigma^2_{T_{ab}}). \quad (26)$$

The distance can then be estimated by combining the two measurements into a single (relatively unambiguous) estimate of the distance. From (25) and (26), observe that for a large data set, this estimator is asymptotically unbiased.

4.3 Analysis of the Phase Error with a Phase-Locked Loop

This subsection analyzes the accuracy of distance measurement in the DEVAPS2 method using a phase-locked loop. A block diagram of the device is shown in Figure 5. A transmitted oscillation is characterized by $A\sin(\omega t + \theta + \psi_{tx}(t))$, which is a pure sinusoid with constant frequency ω, initial phase θ, and frequency fluctuation $\psi_{tx}(t)$. Thus, the input signal may be represented by

$$\begin{aligned} A\sin(\omega t+\theta+\psi_{tx}(t)) &= A\sin(\omega_0 t+\theta_0(t)+\psi_{tx}(t)) \\ &= A\sin(\omega_0 t+\theta_1(t)), \end{aligned}$$

where $\theta_0(t)=(\omega-\omega_0)t+\theta$, $\theta_1(t)=\theta_0(t)+\psi_{tx}(t)$, $(\omega-\omega_0)$ is the difference between the transmitter oscillator frequency ω and the voltage control oscillator (VCO) frequency ω_0, and $\psi_{tx}(t)$ is the frequency instabilities of the transmitter oscillator [49]. The phase of the noisy VCO is

$$\theta_2(t)=\theta_{vco}(t)+\psi_{vco}(t), \tag{27}$$

where

$$\frac{d}{dt}\theta_{vco}(t)=Ke(t), \tag{28}$$

$e(t)$ is the VCO input voltage and $\psi_{vco}(t)$ is the short-term instabilities of the VCO oscillator [49].

We define the total phase error by $\phi(t)=\theta_1(t)-\theta_2(t)$, which is the instantaneous phase error of the VCO with respect to the received signal. [53] shows that the steady-state phase-error distribution for the first-order loop ($F(s)=1$) can be obtained by solving the Fokker-Planck equation in the region $-\pi\le\phi\le\pi$ with appropriate boundary conditions. Here the system analysis can be generalized considering the frequency instabilities of the transmitter oscillator and VCO. The generalized result of the steady-state distribution is given by

$$P(\phi)=c_1\exp(\alpha\cos\phi+\beta\phi)[1+c_2\int_{-\pi}^{\phi}\exp(-\alpha\cos x+\beta x)\,dx] \tag{29}$$

with the boundary condition

$$P(\pi)=P(-\pi) \tag{30}$$

and the normalizing condition

$$\int_{-\pi}^{\pi}P(\phi)\,d\phi=1, \tag{31}$$

where

$$\alpha=\frac{4A}{KN_0}, \tag{32}$$

$$\beta=\frac{4(\omega-\omega_0+\Delta\dot{\psi}(t))}{K^2N_0}, \tag{33}$$

$$\Delta\dot{\psi}(t)=\dot{\psi}_{tx}(t)-\dot{\psi}_{vco}(t) \tag{34}$$

$$c_2 = \frac{\exp(-2\beta\pi) - 1}{\int_{-\pi}^{\pi} \exp(-\alpha \cos x + \beta x)\, dx} \tag{35}$$

from the boundary condition (30), and then c_1 can be obtained by means of (31).

For the general case (i.e. when the VCO quiescent frequency is not tuned to the frequency of the transmitted signal or the difference in the frequency instabilities of the transmitter oscillator and the VCO is not negligible), (29), (31), and (30) represent the entire steady-state phase-error probability density. In order to simplify the analysis, consider the special case which assumes that the frequency offset between the transmitted signal and VCO is zero ($\omega = \omega_0$) and the frequency instabilities of the transmitted oscillation and VCO is very small ($\Delta\dot{\psi}(t) \simeq 0$). Therefore,

$$P(\phi) = \frac{\exp(\alpha \cos \phi)}{2\pi I_0(\alpha)} \quad -\pi \leq \phi \leq \pi \tag{36}$$

with variance

$$\sigma_\phi^2 = \frac{\pi^2}{3} + 4 \sum_{n=1}^{\infty} \frac{(-1)^n I_n(\alpha)}{n^2 I_0(\alpha)}. \tag{37}$$

When α is large ($\alpha > 4$), the linear model without signal modulation can be used to approximate the variance of phase error for the first-order loop with $\omega = \omega_0$. Hence, the variance of phase error is

$$\sigma_\phi^2 = \frac{N_0(AK/4)}{A^2} = \frac{N_0 B_L}{A^2} = \frac{1}{\text{SNR}} = \frac{1}{\alpha}, \tag{38}$$

where $B_L = AK/4$ is the defined loop bandwidth of the first-order filter and α is the SNR.

Sensor A then uses a first-order PLL to measure the phase of the received signal and obtain the phase difference. Following the procedures in the DEVAPS2 method and assuming that the frequency estimation error is negligible, the phase difference is

$$\phi_{PLL}^{(a)} = \frac{n}{m}(2\pi f_1 t_{ab} + \triangle\phi_b) + 2\pi \frac{n}{m} f_1 t_{ab} + \triangle\phi_a, \tag{39}$$

where $\triangle\phi_a$ and $\triangle\phi_b$ are the phase errors in sensor A and sensor B, respectively. Therefore, the estimate of transmission time T_{ab} yields

$$T_{ab} = \frac{m}{4\pi n f_1} \phi_{PLL}^{(a)} \tag{40}$$

$$= t_{ab} + \frac{1}{4\pi f_1}(\triangle\phi_b + \frac{m}{n}\triangle\phi_a). \tag{41}$$

When the SNR is large, (36) is very close to a Gaussian distribution. Hence, the distribution of T_{ab} can be approximated by

$$T_{ab} \sim N(\mu_{T_{ab}}, \sigma_{T_{ab}}^2) \tag{42}$$

with

$$\mu = t_{ab}$$
$$\sigma^2_{T_{ab}} = \frac{n^2 + m^2}{\alpha(4\pi n f_1)^2}.$$

Therefore, the distribution of distance measurement can be described as in (25) and (26).

5 DEVAC vs. DEVAPS: the Trade-offs

Since multiple estimates using the DEVAC method consume the same energy as a single estimate using the DEVAPS method, the accuracy of these two methods can be easily compared.

5.1 Energy Consumption

Assume the transmission path is symmetric and the radio dissipates E_{elec} in the transmitter or receiver circuitry and E_{pro} in the information processing.

Based on the estimation procedures in the DEVAC method, the radio expends:

$$E_{(\text{DEVAC})} = 3E^{(\text{Tx})}_{elec(\text{DEVAC})} + 3E^{(\text{Rx})}_{elec(\text{DEVAC})} + 2E_{pro(\text{DEVAC})} \quad (43)$$
$$= 6E_{elec(\text{DEVAC})} + 2E_{pro(\text{DEVAC})}, \quad (44)$$

where $E^{(\text{Tx})}_{elec(\text{DEVAC})} = E^{(\text{Rx})}_{elec(\text{DEVAC})} = E_{elec(\text{DEVAC})}$ and $2E_{pro(\text{DEVAC})}$ are consumed by the clock calibration and propagation time calculation.

For the DEVAPS method, the radio expends:

$$E_{(\text{DEVAPS})} = 2E^{(\text{Tx})}_{elec(\text{DEVAPS})} + 2E^{(\text{Rx})}_{elec(\text{DEVAPS})} + 2E_{pro(\text{DEVAPS})} \quad (45)$$
$$= 4E_{elec(\text{DEVAPS})} + 2E_{pro(\text{DEVAPS})}, \quad (46)$$

where $E^{(\text{Tx})}_{elec(\text{DEVAPS})} = E^{(\text{Rx})}_{elec(\text{DEVAPS})} = E_{elec(\text{DEVAPS})}$ and $2E_{pro(\text{DEVAPS})}$ are consumed by a PLL or MLE to abstract the phase and frequency information.

Since computation is much cheaper than communication, we have

$$E_{pro(\text{DEVAC})} = i \cdot E_{elec(\text{DEVAC})} \quad (47)$$
$$E_{pro(\text{DEVAPS})} = j \cdot E_{elec(\text{DEVAPS})}, \quad (48)$$

where i and j are ratios of the processing energy consumption to the energy consumption for running the circuitry in respective methods and $0 < i, j < 1$.

For a given energy and from (43) and (45), the relationship between $E_{elec(\text{DEVAC})}$ with k estimates and $E_{elec(\text{DEVAPS})}$ with a single estimate is

$$E_{elec(\text{DEVAC})} = \frac{4+2j}{(6+2i)k} \cdot E_{elec(\text{DEVAPS})}, \tag{49}$$

which implies

$$\text{SNR}_{(\text{DEVAC})} = \frac{4+2j}{(6+2i)k} \cdot \text{SNR}_{(\text{DEVAPS})}, \tag{50}$$

where the SNRs represent the signal-to-noise ratios for the respective methods. Therefore, in order to achieve an acceptable SNR, η, the threshold of the number of estimates k in the DEVAC method is given by

$$k \leq \frac{(4+2j)}{(6+2i)} \cdot \frac{\text{SNR}_{(\text{DEVAPS})}}{\eta}. \tag{51}$$

5.2 Estimation Accuracy

For the DEVAC method, the fundamental limitation on the accuracy of the estimates is related to the form of the signal and the clock, including the signal bandwidth, the signal-to-noise ratio (SNR), and the timing calibration. Assume that the random range error and range bias error from propagation conditions are small and negligible. The range-measurement accuracy may be characterized by the measurement error, σ_R, given by the root-sum-square of the error components.

$$\sigma_R = \left(\sigma_S^2 + \sigma_{clock}^2\right)^{1/2}, \tag{52}$$

where σ_S is the SNR-dependent random range measurement error, which is

$$\sigma_S = \frac{c}{2\beta_e\sqrt{2\text{SNR}}}, \tag{53}$$

where β_e is the effective bandwidth of the signal [40], and σ_{clock} is the clock-dependent random range measurement error, which is $c\sigma_{T_{ab}}$.

With the finite energy constraint and referring to (50), the range-measurement accuracy of the DEVAC method

using k independent estimates is

$$\sigma_R^{(k)} = \left[\frac{1}{k}(\sigma_S^2 + \sigma_{clock}^2)\right]^{1/2} \quad (54)$$

$$= \left[\frac{1}{k}\left(\frac{c^2}{8\beta_e^2 \mathrm{SNR}_{(\mathrm{DEVAC})}} + c^2\sigma_{T_{ab}}^2\right)\right]^{1/2} \quad (55)$$

$$= \left[\frac{(6+2i)c^2}{8\beta_e^2(4+2j)\mathrm{SNR}_{(\mathrm{DEVAPS})}} + \frac{c^2\sigma_{T_{ab}}^2}{k}\right]^{1/2}, \quad (56)$$

where $0 < i, j < 1$. Observe that if the signal bandwidth remains the same for all measurements using the DEVAC method, then the global SNR-dependent random range measurement error of the DEVAC method with multiple measurements does not decrease due to the averaging (i.e. a scale factor $1/\sqrt{k}$) and a lower SNR (i.e. a larger corresponding error $\sqrt{k} \cdot \sigma_S$). This means the σ_S with one estimate applying the finite total energy is identical to the σ_S with the energy constraint and multiple estimates. However, the clock-dependent random range measurement error can be reduced by a scale factor $1/\sqrt{k}$ while using multiple measurements because of the averaging.

On the other hand, the estimation accuracy of the DEVAPS method with the ML estimator relies on the number of samples of the received signal, the SNR, and the carrier frequencies of the signals. The range-measurement accuracy using phase shift information is derived as in (25). The above demonstrates the trade-offs between the accuracy of the distance estimation and the complexity of the circuitry needed for implementation. Therefore, depending on the range-measurement accuracy, these key parameters in each method can be chosen to achieve desired performance. A numerical example of this analysis is illustrated in Section 6.1.

6 Performance Evaluation

This section demonstrates the performance of the various distance measurement methods. Assume that the propagation time is $t_{ab} = 10^{-7}$s (i.e. the true distance is d = 30 m) and with SNR = 3 dB for all distance measurement settings. Note that these settings may represent a reasonable transmission range for many wireless sensor applications as in the emerging ZigBee standard [54].

6.1 Numerical Results

The first set of numerical results evaluates the critical timing parameters t_i^a and t_j^b in the DEVAC method to determine the required level of timing resolution (i.e. the standard deviation of the time measurement σ). Figure 6 (left) shows

the typical performances of time and distance measurement using (10) with the parameters detailed in the caption and the clocks providing a resolution of 1 ns and 100 ns, respectively. Figure 6(a) and 6(b) show the distance as estimated by a single pulse. As expected, a distance measurement with a higher timing resolution has a smaller measurement variance. However, combining the estimates of k pulses allows the less accurate clocking to achieve similar accuracy to the faster clocks. For example, with the parameters as in Figure 6, it would require 10000 pulses for the 100 ns clock to achieve the same estimation accuracy as the 1 ns clock. The DEVAC method illustrates the importance of timing resolution for accurate distance estimation. The drawback is that a clock with high timing accuracy may be expensive.

The second set of numerical results examines the performance of the DEVAPS2 method using phase information. Given a carrier frequency f_1, a mode-locked frequency $f_2 (= \frac{n}{m} f_1)$, and with other parameters as before, Figure 6 (right) shows the performance of the distance measurement using a ML estimator with N samples of the received signal based on (25) and (26). The larger the data set, the smaller the measurement variance. Observe that the performance of the distance measurement with $N = 50$ samples is comparable to the measurement with $N = 500$ samples, even for low SNR. Thus $N = 50$ samples may be sufficient for the asymptotic properties to apply. In order to distinguish the ambiguous estimates, Figure 6 also shows the disambiguation scheme in the DEVAPS2 method using two appropriate transmitted frequencies ($f_1 = 50$ MHz and $f_2 = \frac{9}{14} f_1$). In this case, the correct answer is around 30 meters.

Instead of using a ML estimator, a phase-locked loop may be used to estimate the phase and frequency offsets. The performance of a PLL is compared to that of a ML estimator based on (24) and (42) assuming that the frequency offset $\triangle f$ is negligible and the SNR is large. As shown in Figure 7 (left), the variance of the phase error in the PLL is larger than that of an asymptotically optimal ML estimator given a high SNR (SNR = 10 dB). Note that though the ML estimator has better performance, the computational complexity of the ML estimator may limit its applicability.

The third set of numerical results depicts the trade-offs between the DEVAC and DEVAPS methods by the analysis derived in Section 5. Assume the transmitted waveform of the DEVAC method is a simple rectangular pulse with a zero phase characteristic.

$$a(t) = \text{rect}\left(\frac{t}{t_p}\right), \tag{57}$$

where t_p is the pulse width. Thus, the effective bandwidth β_e is

$$\beta_e = \frac{3}{2t_p}. \tag{58}$$

Given the parameters detailed in the caption, Figure 8 shows the range-measurement accuracy of each method

based on the same energy consumption. Observe that the distance measurement is refined and the clock skew problem is alleviated by multiple estimates such that the performance of the DEVAC method is competitive with that of the DEVAPS method. However, equation (52) for estimation errors in the DEVAC method are derived using the assumption of large SNR, which means there may exist a threshold for the number of estimates k with finite energy constraint; otherwise, equation (54) may result in a poor approximation for estimation error due to small SNR in each estimate.

The fourth set of numerical results examines the performance of the distance measurement using both the received power method and the DEVAPS1 method. In this paper, the free space propagation model is used to predict received signal strength when there exists a line-of-sight path between the transmitter and receiver.

Let the received power in sensor B be:

$$P_{rx} = \frac{KP_{tx}}{D^{\alpha}}, \tag{59}$$

where D is the estimated distance, P_{tx} is the transmitted power, K is a constant related to the transmitter and receiver antenna gains, the system loss factor and the radio wavelength, and α is the attenuation exponent. Due to the log-normal shadowing effects [55],[56], the power measurement P_{rx} is a log-normal random variable

$$f_{P_{rx}} \sim N(\overline{P}_{rx}(\text{dB}), \sigma_{sh}^2), \tag{60}$$

with $\overline{P}_{rx}(\text{dB}) = \overline{P}_{tx}(\text{dB}) - 10\alpha \log_{10}(d)$, where $\overline{P}_{rx}(\text{dB})$ and $\overline{P}_{tx}(\text{dB})$ are the decibel values of the mean received power and the mean transmitted power in sensor B, d is the true distance between sensors A and B, and σ_{sh}^2 is the variance of the log-normal shadowing.

From (59), the estimated distance D can be expressed by

$$D = 10^{\frac{P_{tx}(\text{dB}) - P_{rx}(\text{dB}) + 10\log_{10} K}{10\alpha}} \tag{61}$$

and the distribution of D is

$$f_D \simeq f_{P_{rx}} \cdot \left| \frac{dP_{rx}(\text{dB})}{dD} \right| \tag{62}$$

$$= \frac{10\alpha}{\sqrt{2\pi} D \ln 10 \sigma_{sh}} \exp\left(- \frac{\left(P_{tx}(\text{dB}) - 10\alpha \log_{10} D + 10\log_{10} K - \overline{P}_{rx}(\text{dB})\right)^2}{2\sigma_{sh}^2} \right) \tag{63}$$

Figure 7 (right) shows the performance of the DEVAPS1 method and the distribution in (63) for a single noisy measurement given the true distance $d = 30$ meters, $P_{tx}(\text{dB}) = 2$, $\overline{P}_{rx}(\text{dB}) = -26.53$, $K = 1$, $\alpha = 2$, and

$\sigma_{sh}^2(\mathrm{dB})/\alpha = 2$ [14]. Note that the distributions are peaked away from the true values. Due to the received power scaling, the addition of noise and the shadowing effects cause the estimate to be biased low. In practice, the receiver noise may be large compared with the signal, and so the usefulness of the power method alone is doubtful. However, the power method may be useful as a means of disambiguating the phase measurements for the DEVAPS methods. In certain cases, the 2-ray ground reflection model [57] may be a useful propagation model considering both the direct path and a ground reflection path between the transmitter and receiver. The performance of the power method applied to the 2-ray ground reflection model is presented and discussed in [58].

The final set of numerical results examines the performance of the distance measurement using phase information in different frequency bands (Figure 9). The purpose of this comparison is to find an appropriate frequency range for DEVAPS1 and DEVAPS2. Consider the following frequency bands for ranging applications [59],[60]: (a) Audio ranging systems: 50 Hz $\sim$ 20 KHz; (b) Ultrasound ranging systems: 20 KHz $\sim$ 200 KHz; (c) VHF: 30 MHz $\sim$ 300 MHz; (d) Mobile radio systems: 890 $\sim$ 960 MHz and 1.85 $\sim$ 1.99 GHz. Notice that the ranging estimation using the DEVAPS1 and DEVAPS2 methods may have a large estimation variance while operating in the frequency bands for acoustic ranging systems (Figures 9(a) and 9(b)). On the other hand, when the DEVAPS1 and DEVAPS2 methods are applied in the frequency band for mobile radio systems (Figure 9(d)), it would be difficult to distinguish the best possible distance estimation because of the phase uncertainty and the very short wavelength. Thus, as shown in Figure 9(c), the VHF frequency band may be a good operating frequency range for distance measurement methods using phase shift information.

6.2 Multipath Effects

Figure 10 illustrates the validation of the approximate Gaussian distributions via simulations. For the DEVAC method, the SNR-dependent random range measurement error, σ_S, is assumed to be negligible (i.e the SNR is large). Therefore, the clock-dependent random range measurement error, σ_{clock}, is investigated. For the DEVAPS method, a PLL is used to estimate the phase and frequency offsets. Observe that if there are no other transmission paths besides the LOS path, the theoretical results provide good approximations for the estimated distances. In order to investigate the contributions of multipath to the distance estimations, the following two cases are examined. Note that the channel model is assumed to be a time-invariant 2-ray ground reflection model [57] considering the LOS path with the attenuation factor a_1 and time delay τ_1 and a ground reflection path with the attenuation factor a_2 and time delay τ_2. Assume that the time delay between two paths is $\triangle\tau = \tau_2 - \tau_1 = 36.5$ *n*s.

Suppose that the LOS path is the dominant path. Given the parameters of the channel propagation model, Figure 11 shows that the DEVAC method works fine in this environment, but the DEVAPS method using a PLL gives biased estimations due to the corrupted phase measurements caused by multipath effects.

On the other hand, when the LOS path is significantly attenuated. Figure 11 shows that both methods give biased estimates. These two experiments show that the DEVAC method remains unbiased even with modest multipath while the DEVAPS method returns biased distance estimates when there is multipath interference. Therefore, compared with the DEVAPS method, the DEVAC method may be a better choice for the ranging problem in an environment with modest multipath interference.

7 Conclusion

This paper uses bidirectional signalling to bypass the need for accurate synchronous clocking and provides a detailed mechanism and analysis for practical round-trip time-delay range measurements. In the DEVAC method, an algorithm is proposed to estimate the frequency offset and propagation time, which is critical to accurate distance estimation. In the DEVAPS method, several techniques are presented to remove ambiguity in distance measurements by using different frequencies. Proper setup for the ranging problems using the DEVAC and DEVAPS methods is presented and the measurement techniques are simulated and analyzed to assess the accuracy of the distance estimation. Depending on the measurement accuracy, then the parameters in each technique can be determined to achieve desired performance.

There are several ways this work can be generalized. The DEVAPS methods require phase locking and estimating the phase at the carrier frequencies. Many practical wireless systems, however, perform the bulk of their signal processing at an *intermediate frequency* (IF) which is generated by mixing the received signal with a local oscillator. This ranging problem using IF signals can be solved by modifying the DEVAPS method as detailed in [58].

This paper assumes that there only exists a LOS transmission path between the sensors. In many applications it may be necessary to account for multipath interference in the transmission path. The simulations imply that the DEVAC method remains unbiased with a modest amount of multipath interference and the DEVAPS method becomes biased due to the corrupted phase measurements in multipath environments. The impact of multipath interference on the system performance is investigated further in [58] which considers bi-directional communication utilizing channel estimation and Tomlinson-Harashima (TH) precoding [61] for distance measurement in static multipath channels.

References

[1] A. Savvides, M. Srivastava, L. Girod, and D. Estrin, "Localization in sensor networks," in C. R. Raghavendra, K. M. Sivalingam, and T. Znati, ed. *Wireless Sensor Networks*, Kluwer Academic Publishers, 2004.

[2] R. Iyengar and B. Sikdar, "Scalable and Distributed GPS free Positioning for Sensor Networks," *IEEE International Conference on Communications*, Volume: 1, Pages:338-342, 2003.

[3] T. Kitasuka, T. Nakanishi, and A. Fukuda, "Location Estimation System using Wireless Ad-Hoc Network," *The 5th International Symposium on Wireless Personal Multimedia Communications*, vol.1, pp. 305-309, 2002.

[4] R. Govindan, T. Faber, J. Heidemann and D. Estrin, "Ad hoc Smart Environments," In *Proceedings of the DARPA/NIST Workshop on Smart Environments*, Atlanta, June 1999.

[5] H. Wang, J. Elson, L. Girod, D. Estrin, K. Yao, and L. Vanderberge, "Target Classification and Localization in Habitat Monitoring," in *IEEE Proceedings of the International Conference on Speech and Signal Processing*, pp. II-597-II-600, April, 2003.

[6] A. H. Sayed, A. Tarighat, and N. Khajehnouri, "Network-Based Wireless Location," *IEEE Signal Processing Magazine*, Vol. 22, No. 4, pp. 24-40, July 2005.

[7] N. B. Priyantha, A. Chakraborty, and H. Balakrishnan, "The cricket location- support system," in *Proc. ACMInt. Conf. Mobile Computing Networking (MOBICOM)*, Boston, MA, Aug. 2000, pp. 32-43.

[8] A. Savvides, C. C. Han, and M. B. Srivastava, "Dynamic fine-grained localization in ad-hoc networks of sensors," in *Proc. ACM Int. Conf. Mobile Computing Networking (MOBICOM)*, Rome, Italy, July 2001, pp. 166-179.

[9] A. Savvides, H. Park, and M. Srivastava, "The bits and flops of the N-hop multilateration primitive for node localization problems," in *Proc. ACM Int. Workshop Wireless Sensor Networks and Applications (WSNA)*, Atlanta, GA, Sep. 2002, pp. 112-121.

[10] D. Niculescu and B. Nath, "Ad Hoc Positioning System (APS) using AoA," in *Proc. IEEE Joint Conf. IEEE Computer Communications Societies (INFOCOM)*, San Francisco, CA, USA, Mar. 2003, pp. 1734-1743.

[11] Y. Shang, J. Meng, and H. Shi, "A New Algorithm for Relative Localization in Wireless Sensor Networks," *Proceedings of the 18th International Parallel and Distributed Processing Symposium* 2004.

[12] F. Gustafsson and F. Gunnarsson, "Mobile Positioning using Wirelsss Networks," *IEEE Signal Processing Magazine*, Vol. 22, No. 4, pp. 41-53, July 2005.

[13] A. Nasipuri and K. Li, “A directionality based location discovery scheme for wireless sensor networks,” in *Proc. ACM Int. Workshop Wireless Sensor Networks Applications (WSNA)*, Atlanta, GA, Sep. 2002, pp. 105-111.

[14] N. Patwari, A.O. Hero, III, M. Perkins, N.S. Correal, and R.J. O’Dea, “Relative location estimation in wireless sensor networks,” *IEEE Transactions on Signal Processing*, Volume: 51, Issue: 8, Pages:2137-2148, Aug. 2003.

[15] E. G. Larsson, “Cramer-Rao Bound Analysis of Distributed Positioning in Sensor Networks,” *IEEE Signal Processing Letters*, Vol. 11, No. 3, pp.334-337, March 2004.

[16] A. Catovic and Z. Sahinoglu, “The Cramer-Rao Bounds of Hybrid TOA/RSS and TDOA/RSS Location Estimation Schemes,” *IEEE Communications Letters*, Vol. 8, No. 10, pp.626-628, October 2004.

[17] J. Hightower and et al., “Design and calibration of the SpotON ad-hoc location sensing system,” 2001.

[18] P. Bahl and V. N. Padmanabhan, “RADAR: an in-building RF-based user location and tracking system,” in *Proc. IEEE Joint Conf. IEEE Computer Communications Societies (INFOCOM)*, Tel Aviv, Israel, Mar. 2000, pp. 775-784.

[19] K. Whitehouse; D. Culler, “Calibration as Parameter Estimation in Sensor Networks,” in *Proceeding ACM WSNA* 2002.

[20] H. Elmer and H. Schweinzer, “High resolution ultrasonic distance measurement in air using coded signals,” in *Proceedings of the 19th IEEE IMTC*, pp. 1565-1570, 2002.

[21] L. Girod and D. Estrin, “Robust range estimation using acoustic and multimodal sensing,” in *Proc. IEEE ICIRS* 2001.

[22] J.-Y. Lee and R. A. Scholtz, “Ranging in a Dense Multipath Environment Using an UWB Radio Link,” *IEEE Journal on Selected Areas in Communications*, Vol. 20, No. 9, pp. 1677-1683, December 2002.

[23] C. A. Kent and F. U. Dowla, “Position estimation of transceivers in communication networks,” *IEEE 5th Workshop on Signal Processing Advances in Wireless Communications*, Page(s):561-565, July 2004.

[24] S. Gezici, Z. Tian, et al., “Localization via Ultra-Wideband Radios,” *IEEE Signal Processing Magazine*, Vol. 22, No. 4, pp. 70-84, July 2005.

[25] J. Gibson, “*The Mobile Communications Handbook*,” *IEEE Press* 1999.

[26] G. Sun, J. Chen, et al., “Signal Processing Techniques in Network-Aided Positioning,” *IEEE Signal Processing Magazine*, Vol. 22, No. 4, pp. 12-23, July 2005.

[27] F. Zhao and L. Guibas, *Wireless Sensor Networks: An Information Processing Approach*, Morgan Kaufmann, CA, 2004.

[28] J. Elson and D. Estrin, “Time synchronization for wireless sensor networks,” in *IPDPS Workshop on Parallel and Distributed Computing Issues in Wireless Networks and Mobile Computing*, April 2001.

[29] M. Maroti, et. al, “Radio Interferometric Geolocation,” in ACM SenSys 2005.

[30] R. C. Dixon, “*Spread Spectrum Systems*,” 2nd ed., John Wiley & Sons, 1984.

[31] L. Freitag, M. Grund, et al., “A bidirectional coherent acoustic communication system for underwater vehicles,” *OCEANS ’98 Conference Proceedings*, Volume 1, Page(s):482-486, 1998.

[32] K. Mizui, M Uchida, and M. Nakagawa, “Vehicle-to-vehicle 2-way communication and ranging system using spread spectrum technique,” in *Proc. of IEEE Vehicle Navigation and Information System Conference*, 1994.

[33] D. D. McCrady, et. al, “Mobile Ranging with Low Accuracy Clocks”, *IEEE Trans. on Microwave Theory and Techniques*, pp. 951-957, June, 2000.

[34] Sunwoo Kim, et. al, “Geolocation in Ad Hoc Networks using DS-CDMA and Generalized Successive Interference Cancellation,”, *IEEE Journal on Selected Areas in Communications: Special Issue on Advances in Military Wireless Communications*, vol. 23, no. 5, May 2005.

[35] E.C. Fieller, “The Distribution of the Index in a Normal Bivariate Population,” *Biometrika*, 24:3-4, pp.428-440, 1932.

[36] D.V. Hinkley, “On the Ratio of Two Correlated Normal Random Variables,” *Biometrika*, 56:3, pp.635-639, 1969.

[37] R. Ware and F. Lad, “Approximating the Distribution for Sum of Product of Normal Variables,” the research report of the Mathematics and Statistics department at Canterbury University, 2003. (http://www.math.canterbury.ac.nz/research/ucdms2003n15.pdf.)

[38] V. H. Poor, *An Introduction to Signal Detection and Estimation*, 2nd ed. New York: Springer-Verlag, 1994.

[39] W. S. Burdic, *Radar Signal Analysis*, Prentice-Hall, 1968.

[40] G. R. Curry, *Radar System Performance Modeling*, 2nd ed., Artech House, 2005.

[41] L. E. Franks, “Carrier and Bit Synchronization in Data Communication – A Tutorial Review,” *IEEE Transactions on Communications*, vol. COM-28, no. 8, pp. 1107-1120, August 1980.

[42] Costas, J.P., “Synchronous Communications,” Proceedings of the IRE, Dec. 1956, pp. 1713-1718.

[43] H. Meyr, M. Moeneclaey, and S. A. Fechtel, *Digital Communication Receivers*, Wiley, 1998.

[44] C. R. Johnson, Jr. and W. A. Sethares, *Telecommunication Breakdown: concepts of telecommunications transmitted via software defined radio*, Prentice-Hall, 2004.

[45] A. Pikovsky, M. Rosenblum, J. Kurths, *Synchronization: A Universal Concept in Nonlinear Sciences*, Cambridge University Press, UK., 2001.

[46] D.W. Allan, "The Measurement of Frequency and Frequency Stability of Precision Oscillators," NBS Tech. Note 669, July 1975.

[47] J.A. Barnes, "Models for the Interpretation of Frequency Stability Measurements," NBS Technical Note 683, August 1976.

[48] D.A. Howe, D.W. Allan, and J.A. Barnes, "Properties of Oscillator Signals and Measurement Methods," Time and Frequency Division, National Institute of Standards and Technology.
(http://www.boulder.nist.gov/timefreq/phase/Properties/main.htm)

[49] F.M. Gardner, *Phaselock Techniques*, 2nd ed. Wiley, New York, 1979.

[50] A. Hajimiri and T. Lee, *The Design of Low Noise Oscillators*, Kluwer 1999.

[51] S.M. Kay, "*Modern Spectral Estimation: Theory and Application*," Prentice-Hall, Englewood Cliffs, N.J., 1988.

[52] S.M. Kay, "*Fundamentals of Statistical Signal Processing: Estimation Theory*," Prentice-Hall, Englewood Cliffs, N.J., 1993.

[53] Viterbi, A. J., "Phase-locked loop dynamics in the presence of noise by Fokker-Planck techniques," *Proceedings of IEEE*, vol. 51, pp. 1737-1753, Dec. 1963.

[54] P. Kinney, "ZigBee Technology: Wireless control that simply works," IEEE 802.15.4 Task Group.
(http://www.zigbee.org/en/resources)

[55] D. C. Cox, R. Murray, and A. Norris, "800 MHz Attenuation Measured in and around Suburban Houses," *AT&T Bell Lab. Technical Journal*, Vol.673, No.6, July-August 1984.

[56] R. C. Bernhardt, "Macroscopic Diversity in Frequency Reuse Systems," *IEEE Journal on Selected Areas in Communications*, Vol-SAC 5, pp. 862-878, June 1987.

[57] T. S. Rappaport, *Wireless communications*, Prentice-Hall, Upper Saddle River, NJ, 1996.

[58] C. Y. Wen, "*Distributed Algorithms for Localization and Management in Wireless Ad-Hoc Sensor Networks*," Ph.D. thesis, University of Wisconsin, 2005.

[59] J. C. Joseph, *Electronic Circuit Guidebook: Sensors*, Prompt, 1997.

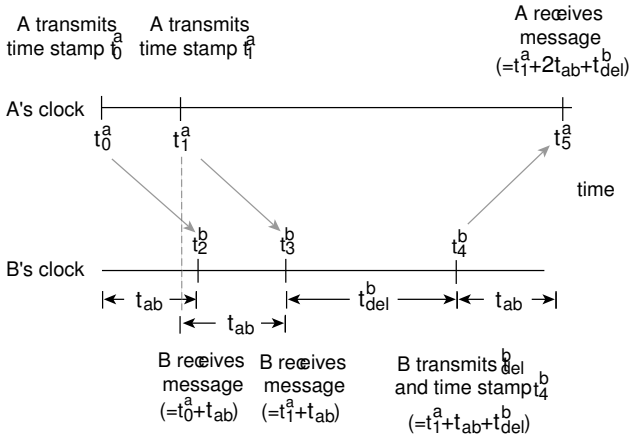

Figure 1: The DEVAC Method: Sensor A receives its reply at t_5^a. This is equal to $t_1^a + 2t_{ab} + t_{del}^b$, from which A can estimate t_{ab} and hence the distance. In this variation, sensor B can calculate the difference between its clock ($t_3^b - t_2^b$) and A's clock using the time stamped information in A's messages ($t_1^a - t_0^a$).

[60] F. Jacob, *Handbook of Modern Sensors*, 2nd ed., Air Press, 1996.

[61] M. Tomlinson, "New Automatic Equalisier Employing Modulo Arithematic," *Electronics Letters*, pp. 138-139, March 1971.

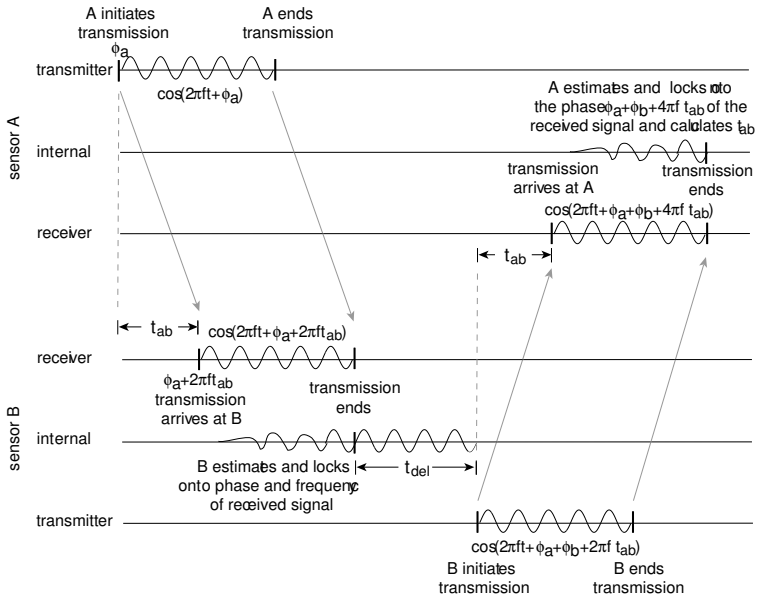

Figure 2: The DEVAPS1 Method: Sensor B receives A's message and locks its phase and frequency to A's carrier. When B replies, A then locks to B's phase. Sensor A can then calculate the phase difference $4\pi f t_{ab}$ and hence estimate the distance between A and B.

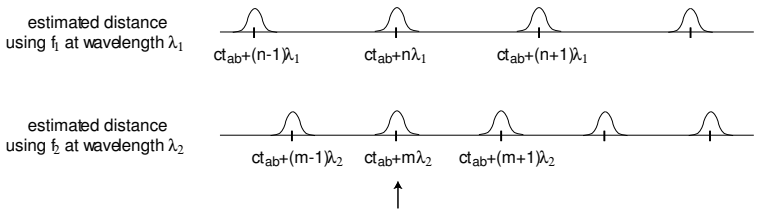

Figure 3: The procedure of Figure 2 is carried out twice, once with carrier f_1 at wavelength λ_1 and once with carrier f_2 at wavelength λ_2. Though each measurement alone is ambiguous, together (along with some a priori knowledge of the order of magnitude of the distances involved), they allow only a small range of likely values, which lie near the arrow.

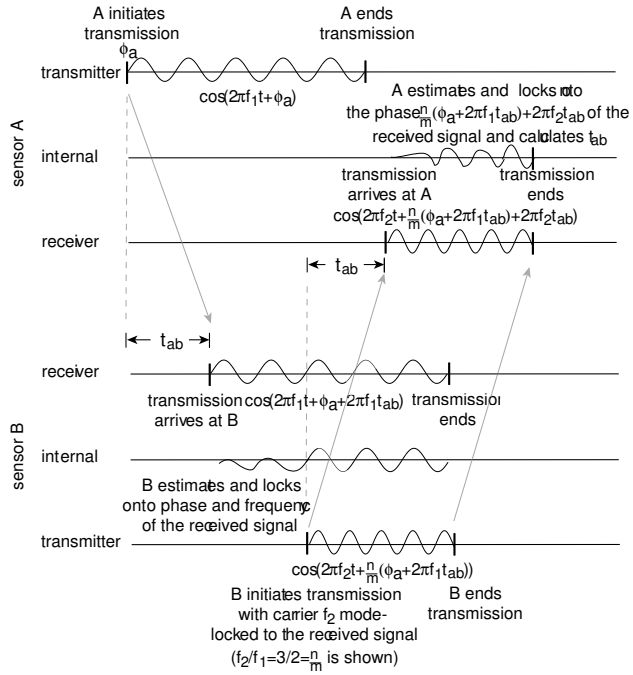

Figure 4: The DEVAPS2 Method: Sensor B receives A's message and locks its phase and frequency to A's carrier. When B replies using carrier f_2 (where f_1 and f_2 are mode locked), A can lock to B's phase. A then calculates the phase difference and estimates the distance between A and B.

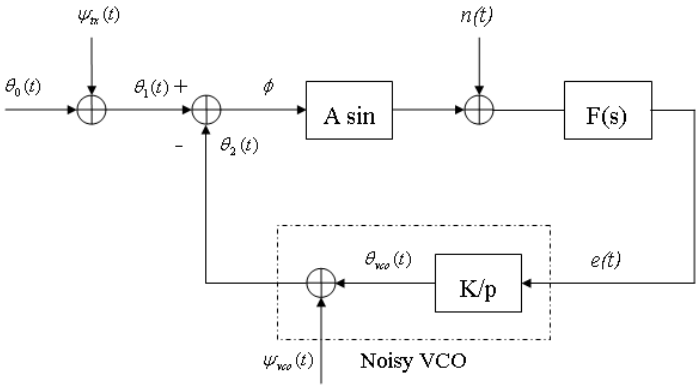

Figure 5: System model of the phase-locked loop.

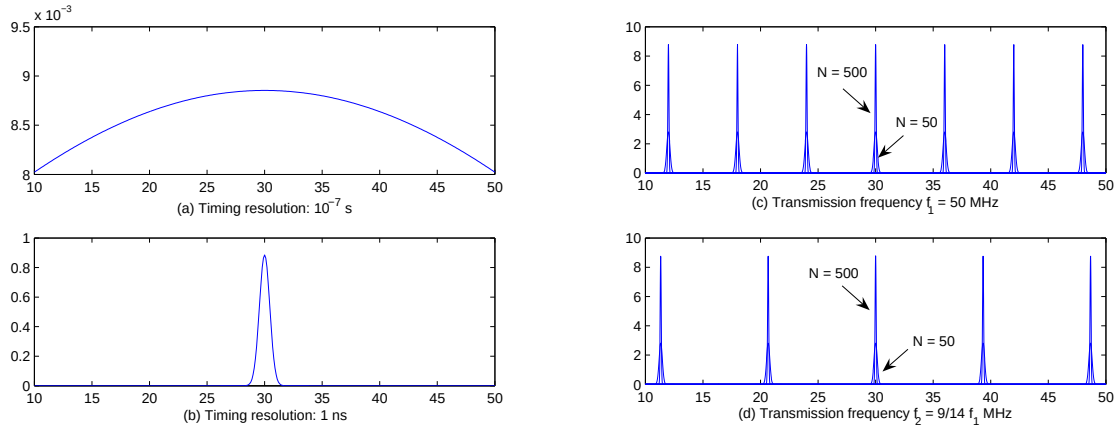

Figure 6: The distribution of distance measurement using the DEVAC Method with a timing resolution of (a) 100 ns and (b) 1 ns: $t_{ab} = 10^{-7}, t_4^b = 3, t_3^b = 2, t_2^b = 1.25, t_1^a = 0.75$, and $t_0^a = 0.25$ (left). The relative pdf of the distance measurement using the DEVAPS2 Method with a ML estimator applied to two different data record lengths, $N = 50$ (larger variance) and $N = 500$ (smaller variance) to estimate the phase at the transmission frequency (c) f_1 = 50 MHz and (d) $f_2 = \frac{9}{14} f_1$.

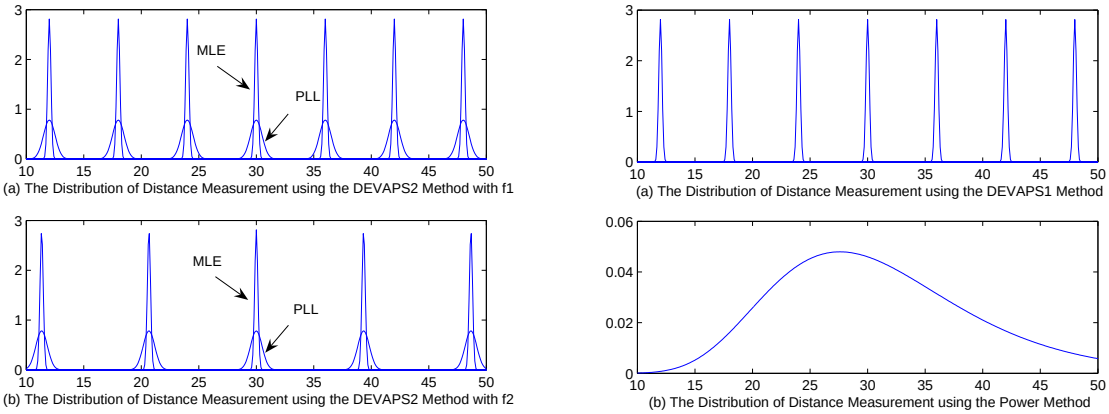

Figure 7: A comparison of the distance measurement using the DEVAPS2 Method with a ML estimator and a PLL (left). The right hand figures show the performance of distance measurement using both the DEVAPS1 method and the power method.

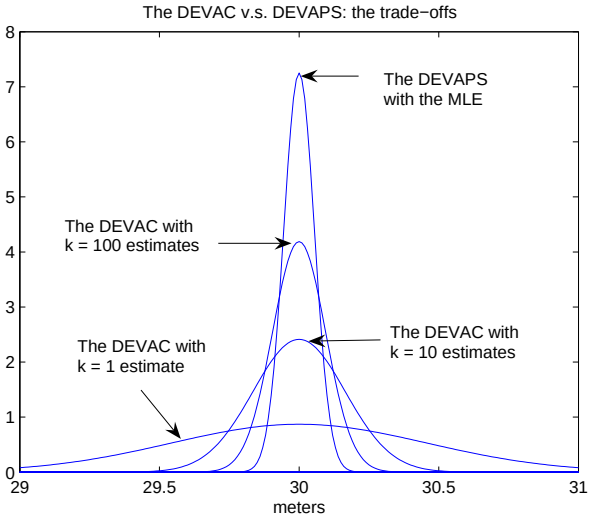

Figure 8: The range-measurement accuracy of the DEVAC and DEVAPS methods based on the same energy consumption with $\mathrm{SNR}_{(\mathrm{DEVAPS})} = 20$ dB, $j = 0.2$, $N = 50$, carrier frequencies $f_1 = 50$ MHz, and $f_2 = \frac{9}{14} f_1$ MHz for the DEVAPS method with a MLE and the pulse width $t_p = 10$ ns, the clock timing accuracy $\sigma = 10$ ns, and $i = 0.1$ for the DEVAC method with varying the number of estimates k = 1, 10, and 100.

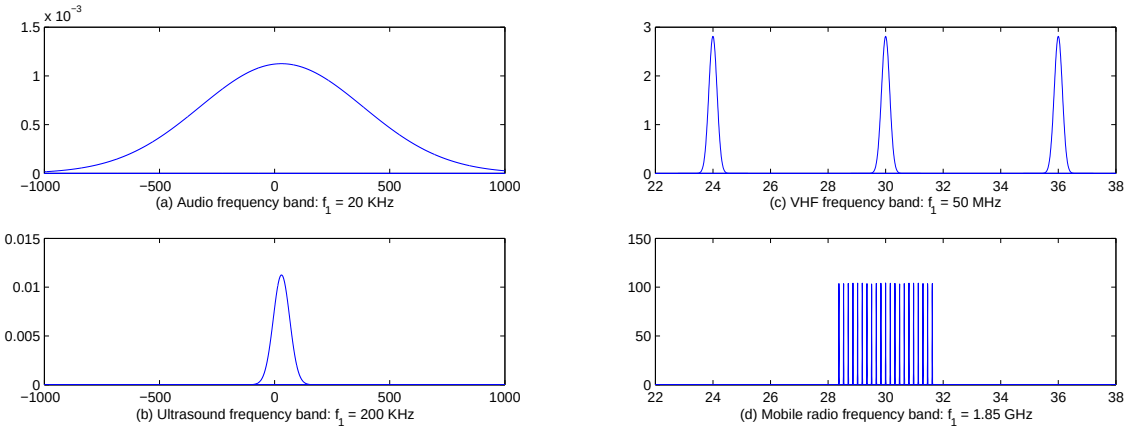

Figure 9: The figures show the relative pdf of the distance measurement using phase information with a ML estimator applying a data record length $N = 50$ to estimate the distance at different frequency bands. The right bottom figure (d) shows an ambiguous distance measurement $ct_{ab} + l\lambda$ with $-10 \leq l \leq 10$.

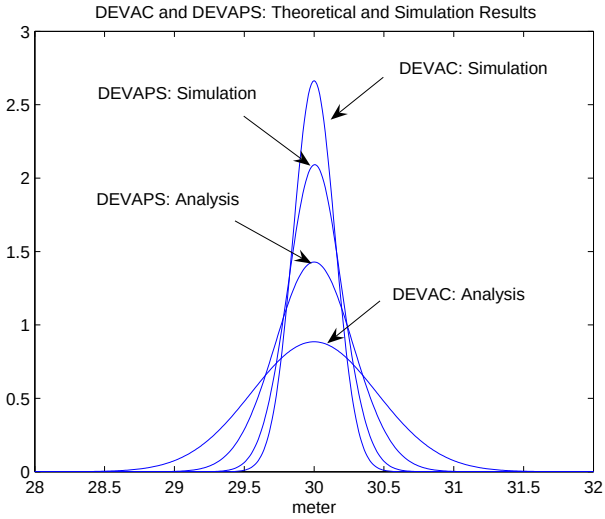

Figure 10: The theoretical and simulation results (1000 typical runs) using the DEVAC method with a timing resolution of 1 ns: $t_{ab} = 10^{-7}, t_4^b = 3, t_3^b = 2, t_2^b = 1.25, t_1^a = 0.75$, and $t_0^a = 0.25$ and the relative pdf of the range measurement using the DEVAPS method with a PLL (SNR = 10 dB) to estimate the phase at the transmission frequency f_1 = 50 MHz and $f_2 = \frac{9}{14} f_1$. The clock skew and channel noise are assumed to be normal random variables with zero means and the standard deviations 10^{-9} and 10^{-2}, respectively.

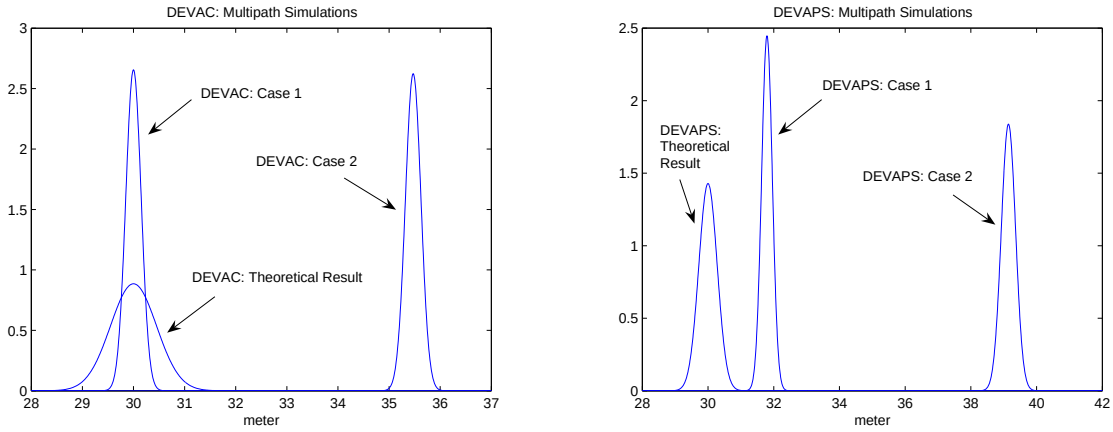

Figure 11: The figures show the relative pdf of the distance measurement in multipath environments via simulations. Case 1 (Dominated by the LOS path): $a_1 = 0.8, a_2 = 0.2, \tau_1 = 0$, and $\tau_2 = 36.5$ *n*s; Case 2 (Dominated by the ground reflection path): $a_1 = 0.2, a_2 = 0.8, \tau_1 = 0$, and $\tau_2 = 36.5$ *n*s.